



Taraxacum-like Mg-Al-Si@porous carbon nanoclusters for electrochemical rutin detection

Nuerbiya Yalikun^{1,2} · Xamxikamar Mamat¹ · Yongtao Li¹ · Xun Hu³ · Ping Wang⁴ · Guangzhi Hu^{1,4}

Received: 22 November 2018 / Accepted: 19 March 2019 / Published online: 27 May 2019
© Springer-Verlag GmbH Austria, part of Springer Nature 2019

Abstract

The authors describe a method for synthesis of a nanomaterial consisting of porous carbon encapsulated Mg-Al-Si alloy (denoted as Mg-Al-Si@PC) nanocluster. The nanocluster was synthesis by a solvothermal reaction, followed by high-temperature annealing. The nanoclusters were used as a novel immobilization platform for electrochemical sensing of rutin. The electrochemical behavior of rutin at a modified electrode was investigated by cyclic voltammetry and differential pulse voltammetry. The modified electrode demonstrates a high electrocatalytic activity toward rutin oxidation at a relatively low working potential (0.6 vs. Ag/AgCl). Under optimal conditions, the sensor has a linear response in the 1–10 μM rutin concentration range, and a 0.01 μM lower detection limit (at an S/N ratio of 3). It was successfully applied to the quantification of rutin in pharmaceutical tablets, and satisfactory results were obtained. Furthermore, the results correspond with those with the standard method and with the amounts indicated by the producer, respectively.

Keywords Cyclic voltammetry · Differential pulse voltammetry · Electrochemistry · Nanocluster · Sensor · Electrochemical response · Electro catalytic oxidation · Flavonoids

Electronic supplementary material The online version of this article (<https://doi.org/10.1007/s00604-019-3369-x>) contains supplementary material, which is available to authorized users.

✉ Xamxikamar Mamat
xamxikmr@aliyun.com

✉ Yongtao Li
yongtao@ms.xjb.ac.cn

✉ Guangzhi Hu
guangzhihu@ms.xjb.ac.cn

¹ Key Laboratory of Chemistry of Plant Resources in Arid Regions, State Key Laboratory Basis of Xinjiang Indigenous Medicinal Plants Resource Utilization, Xinjiang Technical Institute of Physics and Chemistry, Chinese Academy of Science, Urumqi 830011, China

² University of Chinese Academy of Sciences, Beijing 100049, China

³ School of Material Science and Engineering, University of Jinan, Jinan 250022, China

⁴ College of Environmental Science and Engineering, Central South University of Forestry and Technology, Changsha 410004, People's Republic of China

Introduction

Flavonoids are widely distributed in fruits and vegetables. They have great antioxidant capacity and other various health benefits [1–3]. Rutin (3,3',4',5,7-pentahydroxyflavone-3-rhamnoglucoside, RU) is a well-known radical scavenger and strong antioxidant [4]. It is also known as vitamin P. Due to its good biological and physiological properties, it has raised considerable attention in food, clinical drug and cosmetic industries, etc. [5]. Therefore, it is crucial to build a simple approach for detection of rutin content in pharmaceuticals and various real samples. Up to know, there are several methods to detect rutin, such as high performance liquid chromatography (HPLC) [6], chemiluminescence [7], capillary electrophoresis [8], UV-vis spectrophotometers [9], flow injection analysis (FIA) [10], sequential injection analysis [11] and electrochemical method [12]. Among these methods, electrochemical method is regarded as a good applicable, on account of convenient, save time, low cost and detection limy and good sensitivity [13]. Furthermore, rutin is an electroactive molecule, which means that it can be easily oxidized and reduced on surface of working electrodes. The determination of rutin by voltammetric methods has become more hot spots.

Wang et al. [14] have described a new method for electrochemical detection of rutin. A nanocomposite was synthesized by a reduced graphene oxide (RGO) as a template for immobilizing zeolitic imidazolate framework-8 (ZIF-8) crystals loaded with the electrochemical probe Methylene Blue (MB), under the optimal conditions, the sensor has an excellent amperometric response towards rutin, with a 20 nM detection limit (at an S/N ratio of 3). Liu et al. [15] describe a method for electrochemical synthesis of a nanocomposite consisting of carboxylated multi-walled carbon nanotubes, polythionine and platinum nanoparticles (denoted as cMWCNT@pTh@Pt). The composite was placed on a glassy carbon electrode (GCE) to obtain a sensor for simultaneous determination of myricetin and rutin and successfully applied to the simultaneous determination of myricetin and rutin in spiked juice samples, and satisfactory results were obtained.

Carbon materials have high chemical, thermal and structural stability with good biocompatibility. It's widely used in biomedicine fields, redox catalyst, ferrofluid, and wave shielding materials [16, 17]. In order to improve the electrochemical property of carbon materials, it is crucial to synthesize more efficient nanocomposites. Nowadays, carbon-based nanomaterials encapsulated with various kinds of metal nanocrystals are new kind of carbon/metal nanocomposite. Among them, magnesium-aluminum alloys and silicon were more functional material, has a number of unique property, such as excellent magnetic, catalytic properties and superior machinability [18, 19]. The combination of metal alloys and carbon materials has the high adsorption capacities and environmental friendliness [20].

Taraxacum-like Mg-Al-Si@PC nanocluster was successfully synthesized by simple solvo-thermal reaction and followed by the high-temperature annealing method. Afterwards, the glass carbon electrode modifies with Mg-Al-Si@PC nanoclusters and applies for electrochemical detection of rutin. The electrochemical sensor display good electro catalytic activity and sensing property towards rutin with the satisfactory linear range from 1 μM up to 10 μM , with low detection limit of 0.01 μM , good stability and interference ability, which is favorable for practical application of fast quantification of rutin.

Experimental

Apparatus

A CHI-760E electrochemical workstation (Shanghai Chenhua Instrument Co. LTD, China) equipped with a three-electrode system was used. Platinum wire as counter electrode, saturated calomel electrode (SCE) as reference electrode and Mg-Al-Si@PC modified glassy carbon electrode set as working electrode, respectively. Phosphate buffer (PB, 0.1 M, pH = 2.0) was used as electrolyte solution for the rutin detection.

In the cyclic voltammetry (CV) test the working potential set as 0.2–0.9 V (vs. ref. electrode) and scan rate was 100 mV s^{-1} ; differential pulse voltammetry (DPV) performed scan range was from 0.2 V to 0.9 V, and the pulse width and pulse period were 0.05 s and 0.5 s, respectively, and the scanning rate was 100 mV s^{-1} . In all experiment, the reported results for every electrode were the mean of three parallel measurements.

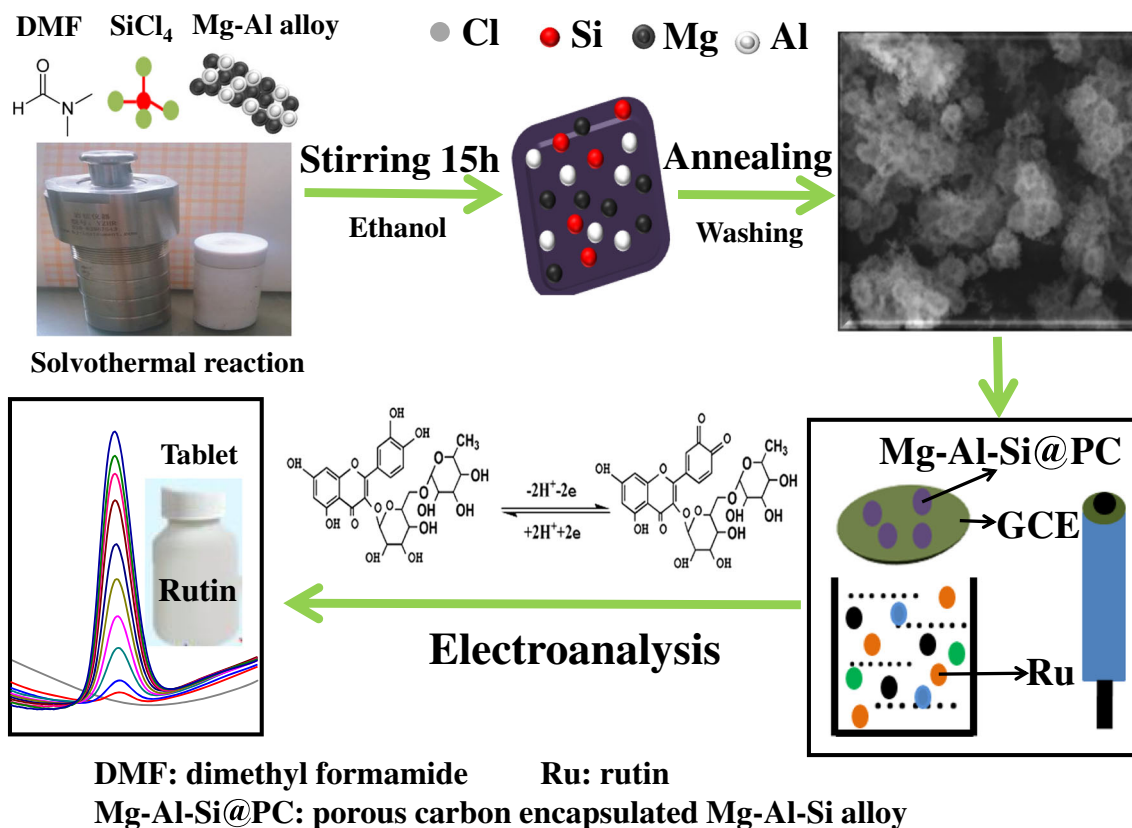
Scanning electron microscope (SEM, Carl Zeiss, Germany), transmission electron microscope (TEM, Titan G2 60–300) were apply to characterization of the micro zone structure of the synthesis nanocomposite. All experiments were carry on the under pure nitrogen bubbling for the aim to remove the interference of dissolved oxygen.

Reagents and materials

The experiment chemicals were analytical grade without any treatment. Glyme, SiCl_4 , Mg-Al alloy powder were purchase from Aldrich, Aladdin Chemicals, 5% Nafion stock solution purchase from Sigma-Aldrich. Rutin was supply by MACKLIN (Shanghai). All aqueous electrochemical testing electrolyte agents were prepare by using deionizer water ($\geq 18.2 \text{ M}\Omega \text{ cm}$). Phosphate buffer with different pH values (from 2.0 to 4.0) were prepared by mixing 0.1 KCl, 0.1 M KH_2PO_4 and 0.1 M K_2HPO_4 and adjusting the pH with HCl or NaOH.

Synthesis of mg-Al-Si@PC nanocluster

Mg-Al-Si@PC nanoclusters were synthesis through the one-pot solvo-thermal reaction and then followed with high-temperature annealing method [7, 21, 22], which was as shown in Scheme 1. The solvo-thermal reaction was performed mixing the a certain amount of Mg-Al alloy powder (0.5–1.0 g) and SiCl_4 (2–3 ml) in N,N-dimethyl formamide (DMF, 30 ml) in a stainless autoclave with teflon liner, then at 170 $^\circ\text{C}$ reaction for 10 h. After cooling to room temperature, the product was immersed in ethanol and kept stirring for 15 h, and then centrifuged (5000 r min^{-1} , 10 min), collected by dried at 90 $^\circ\text{C}$ in vacuum, for 8 h. Afterwards, the composite was treated with annealing at 800 $^\circ\text{C}$ for 2 h, then fast cooling 3 min under Ar flow. The quick cooling of the product may maintain the morphological structure of product. After the product ultrasonic treatment in aqueous solution for 30 min and filtering, subsequently washed for three times with water and ethanol, respectively, then was dried at 80 $^\circ\text{C}$ in vacuum, for 10 h. The particles become highly fluffy [23], due to the removal of MgCl_2 . Moreover, it is not a necessary to use strong acid for the post-treatments, which alleviate serious environmental concerns about the disposal of these acids. The safe and cheap reagents, conventional equipment, and simple operation to prepare porous structured nanoclusters make the synthesis attractive [24, 25].



Scheme 1 Schematic presentation of synthesis process of Mg-Al-Si@PC nonoclusters and electrochemical detection of rutin

Fabrication of working electrode

GCE was usually polished with aluminum slurries (1.0, 0.3 and 0.05 μm), for the purpose to get the mirror-like fresh surface. Sequentially, the GCE wash with (ethanol and deionizer water) under ultrasonication for 30 s to remove the aluminum oxide attached at the GCE surface. Finally, the clean GCE was dry with nitrogen flowing in air. Mg-Al-Si@PC/GCE was prepared by casting 5 μL of the synthesis Mg-Al-Si@PC suspension on the GCE surface and then drying at room temperature.

Results and discussion

Choice of material

Carbon nanomaterials a promising material, have gained widespread attention due to their unique structural properties. Among them, porous carbons offer numerous remarkable properties, such as high specific surface area, high conductivity, chemical stability and tunable surface chemistry. That allows the development of a range of strategies for the introduction of functional groups, and consequently, for the anchoring of metal and metal complexes. The synthesis of Mg-Al-Si@PC is simple, low costs and the precursor of nanoclusters Mg-Al alloy and SiCl₄ were common chemicals, easy to get,

also excellent material for synthesis of functionalized nanocomposite. In addition Mg-Al-Si@PC has the special morphological structure of taraxacum like porous structure. Therefore Mg-Al-Si@PC used as electrode material for electrochemical detection of rutin.

Characterization of Mg-Al-Si@PC nanoclusters

The morphological and structural properties of Mg-Al-Si@PC were characterized by SEM and TEM. SEM image of the Mg-Al-Si@PC confirms that taraxacum like cluster structure with the numerous holes was investigated in Fig. 1a. The further TEM image of the nanocomposite and the related high-angle annular dark field (HAADF) image (Fig. 1b and c) undoubtedly reveal the taraxacum like cluster structure of this material at same. The EELS mapping of the select area in Fig. 1d-1h illustrates that the Mg-Al-Si@PC was consist from aluminum, silicon, magnesium, carbon and oxygen elements. These elements were homogenously distribute in nanoclusters, as shown in Fig. 1 (i) displays the overlay signals in the element map texture.

Electrochemical behavior of modified electrodes

CV of the ferricyanide system is a useful tool to characterize the electrochemical behaviors of the electroactive species on

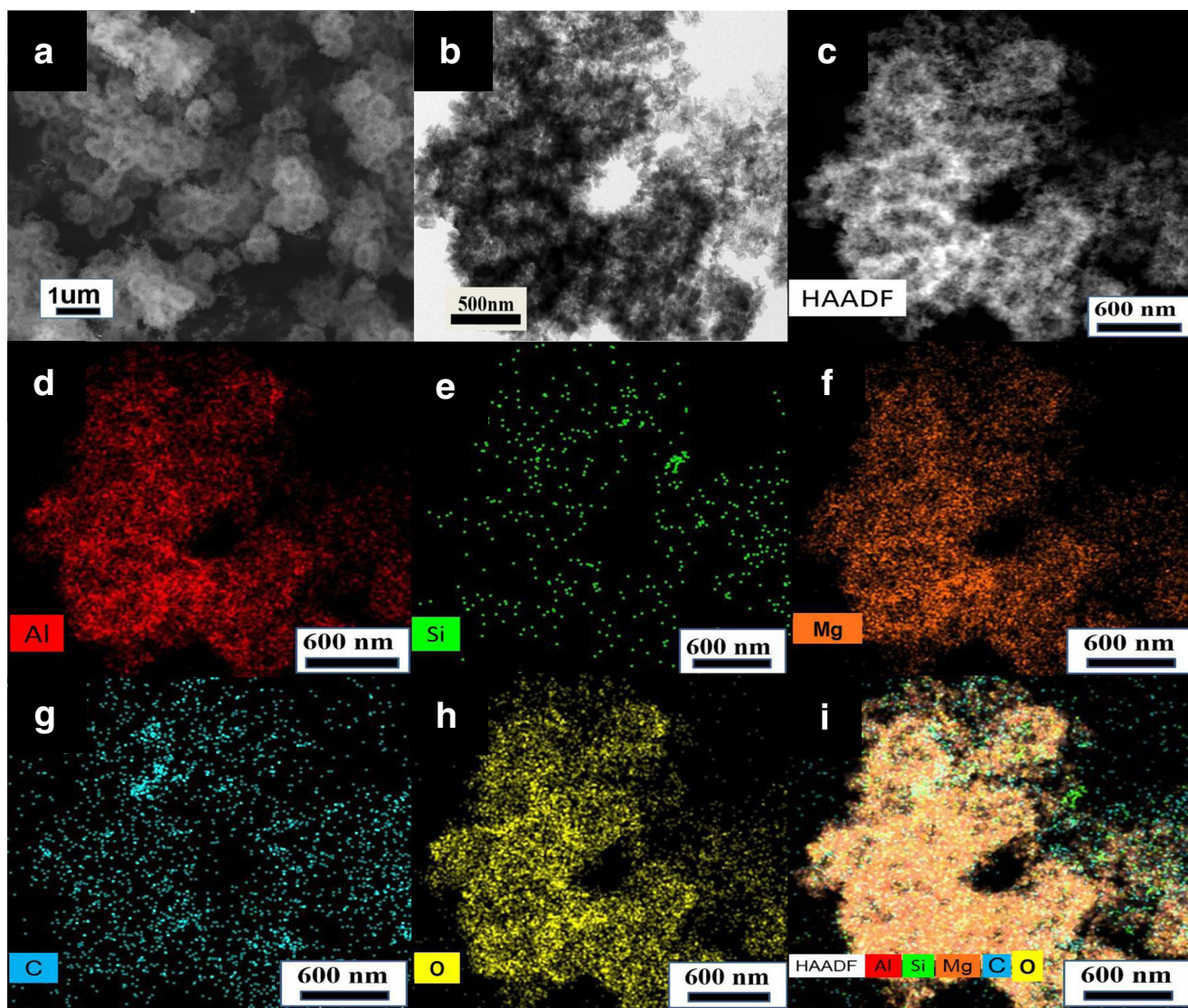


Fig. 1 SEM image of Mg-Al-Si@PC (a); TEM images of Mg-Al-Si@PC (b), (c) high-angle annular dark-field scanning transmission electron microscopy (HAADF-STEM) image of Mg-Al-Si@PC and (d–i) electronic

emitter location system EELS map of aluminum, silicon, magnesium, carbon and oxygen

the modified electrode surface. Figure 2 shows a comparison of the electroactivity among different modified electrodes investigated by CV in 0.1 M KCl solution containing 5 mM $K_3Fe(CN)_6$, at the scan rate 100 mV s^{-1} . For bare GCE (curve a), a couple of well-defined redox peaks are observed with peak-to-peak separation (ΔE_p) of 127 mV. For Mg-Al-Si@PC /GCE (curve b), peak currents increases and the ΔE_p value decreases to 106 mV. The result indicate that the surface property of the Mg-Al-Si@PC /GCE has been significantly changed. This confirms electrocatalytic activity of the Mg-Al-Si@PC /GCE. The available surface area for reaction of species in solution can be calculated by the Randles-Sevcik eq. (1) [26, 27]:

$$I_p = 2.69 \times 10^5 n^{3/2} A D^{1/2} C_0 \nu^{1/2} \quad (1)$$

Where, I_p is the peak current in A. C_0 is the concentration of the electroactive species (mol cm^{-3}), n is the number of electrons

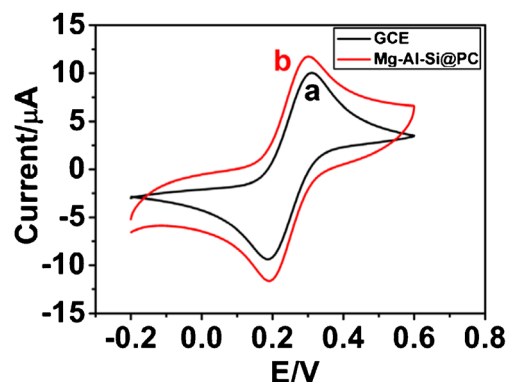


Fig. 2 CV curves of bare GCE (a) and Mg-Al-Si@PC/GCE (b) in 0.1M KCl solution containing 1 mM $K_3Fe(CN)_6$. Scan rate = 100 mV s^{-1}

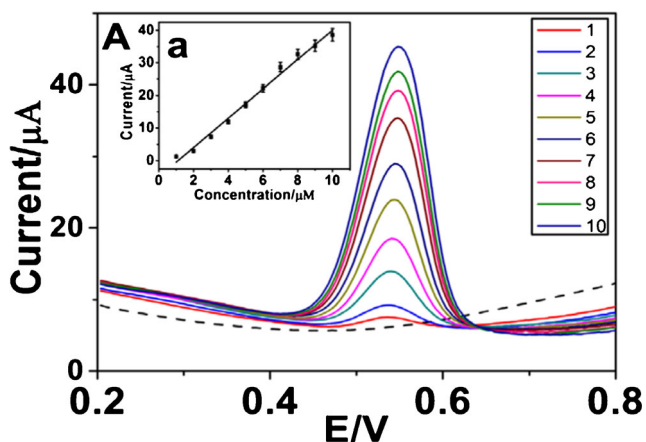


Fig. 3 A: DPV curves of Mg-Al-Si@PC/GCE with different rutin concentrations (0, 1, 2, 3, 4, 5, 6, 7, 8, 9, 10 μM) in phosphate buffer of pH = 2.0, Scan rate = 100 mV s^{-1} . a: The plots of the oxidation currents versus the rutin concentration

involved, D is the diffusion coefficient ($\text{cm}^2 \text{S}^{-1}$), ν is the scan rate (V s^{-1}) and A is the electroactive surface area (cm^2). For Mg-Al-Si@PC /GCE the electroactive surface area is maximum (0.028cm^2) as compared with bare GCE (0.015cm^2).

Electrochemical determination of rutin by using different electrodes

The electrochemical behavior of the prepared material towards rutin was surveyed by voltammetric method such as cyclic voltammetry (CV) in phosphate buffer of pH = 2.0 containing 10 μM rutin. Electrochemical behavior of rutin at bare GCE and Mg-Al-Si@PC modified electrode is displayed in Fig. S1 (in Electronic Supporting Material). CV scan survey showed that bare GCE performed a pair of weak redox peaks (curve a), the redox peak potential appear at 562mV (E_{pa}) and 543 mV (E_{pc}), (vs.SCE). The redox peak currents were located as 4.03 μA and 3.122 μA for I_{pa} and I_{pc} respectively, the ratio of $I_{\text{pa}}/I_{\text{pc}}$ was calculated to be 1.32. While for the Mg-Al-Si@PC modified electrode, pair of visible redox peaks was observed, showing the sensor has better electrochemical response towards rutin. The anodic peak potential and cathodic peak potential was 576 mV and 531 mV, respectively (vs. SCE). The I_{pa} was 20.52 μA and the I_{pc} was 16.37 μA , which were 5 fold higher than unmodified GCE. The ratio of redox peak current ($I_{\text{pa}}/I_{\text{pc}}$) was calculated to be 1.25, cathode branch and the anode branch were nearly coincident, indicating more reversible electrochemical redox process of rutin on the modified electrode [9]. The results indicate that, the synthesis Mg-Al-Si@PC nanoclusters can act as a more effective medium for promoting electrochemical redox of rutin. Therefore the Mg-Al-Si@PC modified electrode shows better electrochemical sensing property towards rutin determination.

Electrochemical parameters of rutin at Mg-Al-Si@PC/GCE

It's well-known that the scanning rate affects the oxidation peak current of rutin at Mg-Al-Si@PC/GCE. So, the effect of scan rates on rutin redox currents were firstly investigated with Mg-Al-Si@PC/GCE by CV technique. It can be seen from the Fig. S2 (in Electronic Supporting Material), the peak current increased gradually by increasing of scan rates, and then peak currents are proportional with the scan rate of potential range. This indicates that the electrode process of rutin at Mg-Al-Si@PC/GCE surface are a adsorption-controlled process [28], this attributed to the large surface area of the modified electrode. The linear regression equations are expressed as $I_{\text{pa}}(\mu\text{A}) = 0.164V(\text{mV s}^{-1}) - 1.923$, ($R = 0.999$) and $I_{\text{pc}}(\mu\text{A}) = -0.134V(\text{mV s}^{-1}) + 1.758$ ($R = 0.999$). With the increasing of scan rate, the oxidation peak potential of rutin positively shifts while the reduction peak potential negatively shifts, resulting in the increasing of ΔE_{p} value. The relationship of the redox peak potentials with $\ln \nu$ were further obtained with two linear regression equations as $E_{\text{pa}}(\text{V}) = 0.016\ln \nu (\text{mV s}^{-1}) + 0.506$ ($R = 0.996$) and $E_{\text{pc}}(\text{V}) = -0.012\ln \nu (\text{mV s}^{-1}) + 0.583$ ($R = 0.992$). Based on Laviron's equation, the slope of the line for E_{pa} and E_{pc} can be expressed as $RT/(1-a)nF$ and $-RT/anF$, respectively. The specific calculation formulas as follows (2–4):

$$E_{\text{pa}} = E^{0'} + \frac{RT}{(1-a)nF} \ln \nu \quad (2)$$

$$E_{\text{pc}} = E^{0'} - \frac{RT}{anF} \ln \nu \quad (3)$$

$$\nu \nu \lg k_s = a \lg(1-a) + (1-a) \lg a - \lg \frac{RT}{nF \nu} - a(1-a) \frac{nF \Delta E_{\text{p}}}{2.303RT} \quad (4)$$

Where (a) is electron-transfer coefficient, (n) is number of electron transfer, (ν) is scan rate, (k) is apparent heterogeneous electron transfer rate constant, (ΔE_{p}) is peak-to-peak potential separation, (F) is Faraday's constant, (R) and (T) represent their usual meaning. According to linear regression equations from $\ln \nu$ and E_{p} , (n) and (a) were calculated to be 2 and 0.57, respectively, based on eq. (4), when the scan rate was 100 mV s^{-1} , the (k_s) was calculated to be 1.56. It can be concluded that a $2e^-$ transfer were involved in electrochemical reaction [29].

The effect of the acidity of the buffer solution on peak current of rutin also tested by differential pulse voltammetry (DPV) in phosphate buffer containing 10 μM rutin, as shown in Fig. S3 (in Electronic Supporting Material). When increasing pH value from 2.0 to 4.0, the oxidation peak current of rutin decrease and peak potentials negatively shifted, indicating that protons take part in reaction [30]. The linear regression equation of oxidation peak potential was obtained as

$E_{pa} = -0.059\text{pH} + 0.681$ ($R = 0.991$) a slope of -59 mVpH^{-1} was the same as the Nernst system of -59 mV/pH at 25°C , demonstrate that an equal number of protons and electrons took part in the electrochemical redox process [31]. At pH 2.0 buffer has a high concentration of protons, this can be increases the electrode reaction. In addition, maximum peak current was appear at pH 2.0, and then was decrease with further increase of pH value, considering that the general situation pH 2.0 was select in the test. It can be inferred that the redox mechanism of rutin at the Mg-Al-Si@PC/GCE is illustrated in Fig. S4.

The effect of the accumulation time towards detection of rutin was shown in Fig. S5 (in Electronic Supporting Material), as can be seen from Fig. S5 the redox peak currents of the rutin increased rapidly with the increase of the incubation time in beginning and reached maximum at 180 s, indicating that the adsorption equilibrium is reached. Therefore, 180 s was chosen as optimal time for rutin analysis [32].

DPV determination of rutin

The electrochemical sensing performance of the Mg-Al-Si@PC/GCE towards rutin was carried out by DPV under optimal conditions. As shown in Fig. 3, the oxidation peak current (I_p , μA) of rutin increased with increasing rutin concentration and the I_{pa} was linearly dependent to the rutin concentration (c , μM) from $1.0 \mu\text{M}$ to $10 \mu\text{M}$. The linear regression equations was described as follows: $I_p (\mu\text{A}) = 4.212C (\mu\text{M}) - 1.228$ with a linear correlation coefficient of 0.991. Based on the signal-to-noise ratio of 3 ($S/N = 3$), the detection limit is calculated to be $0.01 \mu\text{M}$.

Table 1 summarizes the comparison of the electrochemical performance of the Mg-Al-Si@PC/GCE with other reported electrochemical methods for rutin determination. The modified electrode show a reasonable linear range and the detection

limit was lower than or equal to most of the previous reports, which can be attributed to the current nanomaterial with highly porous structure, high surface area and good electro-conductivity. In addition, the fabrication of our nanomaterial sensor was more controllable and convenient through the strategy of electrochemical synthesis.

Interferences study

To investigate the interference performance of the proposed electrochemical sensor, selectivity study was investigated by introducing other interfering compounds while the rutin concentration was fixed to $10 \mu\text{M}$. The limit of potential interfering substances was defined as $\pm 5\%$ relative error in the determination of rutin. The results were showed in Table S1 (in Electronic Supporting Material). The result indicates that various potentially interfering ions have tiny influences to the signals of the rutin (signal change less than 5%, $n = 3$). In addition, in the electrochemical test, appear the response currents for small drug molecules (ascorbic acid, glucose, dopamine, uric acid) and luteolin, indicate that the analytical method had good selectivity and can be applied for the electrochemical detection of some other flavonoids and small drug molecules.

Reproducibility and stability of the modified electrode

The reproducibility and stability of the modified electrode are the important characteristics for the future application. The reproducibility of the electrochemical sensor was evaluated by detecting rutin through CV method for ten times under the same testing condition. The relative standard deviation (R.S.D) is calculated to be 4.63%, indicating that the electrode is highly reproducible. The stability was investigating through

Table 1 Comparison of analytical parameters of different modified electrodes for rutin analysis

Modified electrodes	Methods	Linear range (μM)	LOD (μM)	Reference
Au-Ag NTs ¹ /NG ²	DPV	0.1 to 420	0.015	[33]
IL ³ -CPE ⁴	CV	0.05 to 100	0.035	[9]
Nafion-GO ⁵ -IL /CILE ⁶	DPV	0.08–100	0.016	[34]
PdAu@RGO ⁷ /GCE ⁸	DPV	0.025 to 5.625	0.025	[35]
GR ⁹ /AuNPs ¹⁰ /AN ¹¹	DPV	0.08 to 10.0	0.025	[36]
NiCo ₂ O ₄ /rGO/GCE	DPV	0.1 to 150	0.01	[37]
PtNPs ¹² /RGO/GCE	DPV	0.05 to 10	0.01	[38]
cMWCNT@pTh@Pt ¹³ /GCE	DPV	0.01 to 15	0.0017	[15]
Fe ₂ O ₃ /RGO ¹⁴ /GCE	DPV	0.015 to 18	0.0098	[32]
Mg-Al-Si@PC/GCE	DPV	1–10	0.01	This work

¹ Nanothorns, ² N-doped graphene, ³ Ionic liquid, ⁴ carbon past electrode, ⁵ graphene oxide, ⁶ carbon ionic liquid electrode, ⁷ reduced graphene oxide, ⁸ glassy carbon electrode, ⁹ graphene, ¹⁰ gold nano particles, ¹¹ acupuncture needle, ¹² platinum nano particles, ¹³ carboxylated multi-walled carbon nanotubes, polythionine and platinum nanoparticles, ¹⁴ reduced graphene oxide

a common process by storing the modified electrode at a 4 °C refrigerator for a week and then used for test its sensing performance towards rutin again; the result revealed that the peak currents of rutin still remained similar to their initial values. Hence, the sensor shows the stability for rutin analysis.

Analytical application

In order to verify the application of the this method, the troxerutin tablet (label amount of 20 mg per tablet, C151104, Yabao Pharmaceutical Group Co. Ltd., China) was detected with the optimal experimental procedure. Before the measurement, a certain number of drug tablets were ground into powder, and then the powder was accurately weigh, subsequently dissolved in ethanol prepared for stock solution. In the test, the appropriate volume of stock solution was diluted with phosphate buffer of pH = 2. It can be seen from the Table S2 (in Electronic Supporting Material), the recovery was calculated as range from 99.8–100.6%, indicate that the standard addition method for rutin detection more visible. In the same, in order to proof the accuracy of the this method, HPLC was apply to the detection of rutin in real samples, the rutin contents were detected for 20.0 ± 0.08 mg per tablet for the troxerutin tablet, which were closed to the result of electrochemical method, so it suggests that Mg-Al-Si@PC/GCE is suitable for the testing for rutin in commercial pharmaceutical samples. However, the current method is not suitable for rutin detection in both body fluids and food samples like juice, owing to thousands of complicated components such as biological macromolecules, small molecules, and high-concentration inorganic salts that coexist in these samples. There for further pretreatments are necessary for these real body fluids and food samples before they can be subjected to rutin detection.

Conclusions

An electrochemical sensor based on the use of Mg-Al-Si@PC nanoclusters is successfully fabricated for the sensitive detection of rutin. The sensor exhibits excellent electro catalytic ability for the sensitive detection of rutin due to the special structure (porous structure) and synergetic effect of the Mg, Al, Si atoms and porous carbon (superior electrical conductivity, good electro catalytic performance and excellent electron transfer mediator). The electrochemical sensor has good analytical performance for rutin with wide linear range, lower LOD, excellent reproducibility selectivity and stability. The modified electrode is further used to analyze rutin in tablet samples with excellent practical abilities. These results indicate that the Mg-Al-Si@PC sensor may have great potential applications in electrochemical sensing.

Acknowledgements This work was supported by West Light Foundation of Chinese Academy of Sciences (2016-YJRC-1), Xinjiang International Science and Technology Cooperation Program (20166010), the National Natural Science Foundation of China (21677171).

Compliance with ethical standards The author(s) declare that they have no conflict of interest.

References

- Arvand M, Farahpour M, Ardaki MS (2018) Electrochemical characterization of in situ functionalized gold organosulfur self-assembled monolayer with conducting polymer and carbon nanotubes for determination of rutin. *Talanta* 176:92–101. <https://doi.org/10.1016/j.talanta.2017.08.012>
- Wang B, Gui R, Jin H, He W, Wang Z (2018) Red-emitting BSA-stabilized copper nanoclusters acted as a sensitive probe for fluorescence sensing and visual imaging detection of rutin. *Talanta* 178: 1006–1010. <https://doi.org/10.1016/j.talanta.2017.08.102>
- Dubey NK, Dubey NK (2015) Plants as a source of natural antioxidants: 110–120. <https://doi.org/10.1079/978178642666.0000>
- Tesio AY, Robledo SN, Granero AM, Fernández H, Zon MA (2014) Simultaneous electroanalytical determination of luteolin and rutin using artificial neural networks. *Sens Actuators B Chem* 203:655–662. <https://doi.org/10.1016/j.snb.2014.07.005>
- Miao Y, Zhang Z, Yan G, Zhang Q, Yan G (2014) Self-assembly of manganese doped zinc sulfide quantum dots/CTAB nanohybrids for detection of rutin. *Biosens Bioelectron* 52:271–276. <https://doi.org/10.1016/j.bios.2013.08.011>
- Attia TZ (2016) Simultaneous determination of rutin and ascorbic acid mixture in their pure forms and combined dosage form. *Spectrochim Acta A Mol Biomol Spectrosc* 169:82–86. <https://doi.org/10.1016/j.saa.2016.06.030>
- Zheng X, Chen X, Chen J, Zheng Y, Jiang L (2016) Synthesis and application of highly dispersed ordered mesoporous silicon-doped Pd-alumina catalyst with high thermal stability. *Chem Eng J* 297: 148–157. <https://doi.org/10.1016/j.cej.2016.03.146>
- Al-Taweel AM, Abdel-Kader MS, Fawzy GA, Perveen S, Maher HM, Al-Zoman NZ, Al-Shehri MM, Al-Johar H, Al-Showiman H (2015) Isolation of flavonoids from *Delonix elata* and determination of its rutin content using capillary electrophoresis. *Pak J Pharm Sci* 28:1897–1903. <https://doi.org/10.1016/71.0000.1501.5568>
- Sun W, Yang M, Li Y, Jiang Q, Liu S, Jiao K (2008) Electrochemical behavior and determination of rutin on a pyridinium-based ionic liquid modified carbon paste electrode. *J Pharm Biomed Anal* 48:1326–1331. <https://doi.org/10.1016/j.jpba.2008.09.014>
- Lu Y, Gao B, Chen P, Charles D, Yu L (2014) Characterisation of organic and conventional sweet basil leaves using chromatographic and flow-injection mass spectrometric (FIMS) fingerprints combined with principal component analysis. *Food Chem* 154:262–268. <https://doi.org/10.1016/j.foodchem.2014.01.007>
- Legnerová Z, Šatinský D, Solich P (2003) Using on-line solid phase extraction for simultaneous determination of ascorbic acid and rutin trihydrate by sequential injection analysis. *Anal Chim Acta* 497:165–174. <https://doi.org/10.1016/j.aca.2003.07.007>
- Qian X, Zhang Q, Zhang Y, Tu Y (2010) Separation/determination of flavonoids and ascorbic acid in rat serum and excrement by capillary electrophoresis with electrochemical detection. *Anal Sci* 26:557–560. <https://doi.org/10.2116/analsci.26.557>
- Sayed Mehdi G, Mohsen B, Mahshid G (2012) Simultaneous determination of sunset yellow and Tartrazine in soft drinks using gold

- nanoparticles carbon paste electrode. *Food Chem* 132:637–641. <https://doi.org/10.1016/j.foodchem.2011.10.103>
14. Wang Z, Yu G, Xia J, Zhang F, Liu Q (2018) One-step synthesis of a methylene blue@ZIF-8-reduced graphene oxide nanocomposite and its application to electrochemical sensing of rutin. *Mikrochim Acta* 185:279. <https://doi.org/10.1007/s00604-018-2796-4>
 15. Liu C, Huang J, Wang L (2018) Electrochemical synthesis of a nanocomposite consisting of carboxy-modified multi-walled carbon nanotubes, polythionine and platinum nanoparticles for simultaneous voltammetric determination of myricetin and rutin. *Mikrochim Acta* 185:414. <https://doi.org/10.1007/s00604-018-2947-7>
 16. Chi Y, Chen Y, Hu C, Wang Y, Liu C (2017) Preparation of mg-Al-Ce triple-metal composites for fluoride removal from aqueous solutions. *J Mol Liq* 242:416–422. <https://doi.org/10.1016/j.molliq.2017.07.026>
 17. Lung YF, Sun YS, Lin CK, Uan JY, Huang HH (2016) Synthesis of mg-Fe-cl hydroxalite-like nanoplatelets as an oral phosphate binder: evaluations of phosphorus intercalation activity and cellular cytotoxicity. *Sci Rep* 6:32458. <https://doi.org/10.1038/srep32458>
 18. Zhang CF, Cao W, Fan TX, Zhang D (2007) Fabrication and formation mechanism of in situ AlN and Mg₂Si particles-reinforced mg matrix composites. *Key Eng Mater* 351:151–155. <https://doi.org/10.4028/www.scientific.net/KEM.351.151>
 19. Leng J, Kang N, Wang DY, Falkenhagen J, Thünemann AF, Schönhals A (2017) Structure–property relationships of nanocomposites based on Polylactide and layered double hydroxides – comparison of MgAl and NiAl LDH as Nanofiller. *Macromol Chem Phys* 218: 1700232. <https://doi.org/10.1002/macp.201700232>
 20. Zhu HT, Ge HY, Jiao SC (2014) Synthesis and catalytic performance of Fe-mg-Al Hydroxalite-like compounds. *Adv Mater Res* 864–867:679–683. <https://doi.org/10.4028/www.scientific.net/AMR.864-867.679>
 21. Jenisha Barnabas M, Parambadath S, Ha C-S (2017) Amino modified core–shell mesoporous silica based layered double hydroxide (MS-LDH) for drug delivery. *J Ind Eng Chem* 53:392–403. <https://doi.org/10.1016/j.jiec.2017.05.011>
 22. Joseph J, Singh SG, Vanjari SRK (2017) Ultra-smooth E-beam evaporated amorphous silicon thin films – a viable alternative for PECVD amorphous silicon thin films for MEMS applications. *Mater Lett* 197:52–55. <https://doi.org/10.1016/j.matlet.2017.03.158>
 23. Furukawa Y, Matsushita Y (2017) Analysis of single and composite structural defects in pure amorphous silicon: a first-principles study. *J Non-Cryst Solids* S00223093173033824 473:64–73. <https://doi.org/10.1016/j.jnoncrysol.2017.07.031>
 24. Lin L, Xu X, Chu C, Majeed MK, Yang J (2016) Mesoporous amorphous silicon: a simple synthesis of a high-rate and long-life anode material for lithium-ion batteries. *Angew Chem Int Ed Engl* 55:14063–14066. <https://doi.org/10.1002/anie.201608146>
 25. Dai F, Zai J, Yi R, Gordin ML, Sohn H, Chen S, Wang D (2014) Bottom-up synthesis of high surface area mesoporous crystalline silicon and evaluation of its hydrogen evolution performance. *Nat Commun* 5:3605. <https://doi.org/10.1038/ncomms4605>
 26. Ganesh PS, Kumara Swamy BE (2015) Simultaneous electroanalysis of hydroquinone and catechol at poly(brilliant blue) modified carbon paste electrode: a voltammetric study. *J Electroanal Chem* 756:193–200. <https://doi.org/10.1016/j.jelechem.2015.08.027>
 27. Ganesh PS, Kumara Swamy BE (2016) Voltammetric investigation of catechol and hydroquinone at triton X-100 modified carbon paste electrode: *Analytical and Bioanalytical Electrochemistry* 8:5: 615–628. [10.1155/2016/8092860](https://doi.org/10.1155/2016/8092860)
 28. Chen X, Yang G, Feng S, Shi L, Huang Z, Pan H, Liu W (2017) Au@AuPt nanoparticles embedded in B-doped graphene: a superior electrocatalyst for determination of rutin. *Appl Surf Sci* 402:232–244. <https://doi.org/10.1016/j.apsusc.2017.01.087>
 29. Sun W, Wang Y, Gong S, Cheng Y, Shi F, Sun Z (2013) Application of poly(acridine orange) and graphene modified carbon/ionic liquid paste electrode for the sensitive electrochemical detection of rutin. *Electrochim Acta* 109:298–304. <https://doi.org/10.1016/j.electacta.2013.07.124>
 30. Liu M, Deng J, Chen Q, Huang Y, Wang L, Zhao Y, Zhang Y, Li H, Yao S (2013) Sensitive detection of rutin with novel ferrocene benzyne derivative modified electrodes. *Biosens Bioelectron* 41: 275–281. <https://doi.org/10.1016/j.bios.2012.08.040>
 31. Li S, Yang B, Wang C, Wang J, Feng Y, Yan B, Xiong Z, Du Y (2017) A facile and green fabrication of Cu₂O-au/NG nanocomposites for sensitive electrochemical determination of rutin. *J Electroanal Chem* 786:20–27. <https://doi.org/10.1016/j.jelechem.2017.01.001>
 32. Liu Z, Xue Q, Guo Y (2017) Sensitive electrochemical detection of rutin and isoquercitrin based on SH-beta-cyclodextrin functionalized graphene-palladium nanoparticles. *Biosens Bioelectron* 89: 444–452. <https://doi.org/10.1016/j.bios.2016.04.056>
 33. Yang B, Bin D, Zhang K, Du Y, Majima T (2018) A seed-mediated method to design N-doped graphene supported gold-silver nanohorns sensor for rutin detection. *J Colloid Interface Sci* 512: 446–454. <https://doi.org/10.1016/j.jcis.2017.10.082>
 34. Hu S, Zhu H, Liu S, Xiang J, Sun W, Zhang L (2012) Electrochemical detection of rutin with a carbon ionic liquid electrode modified by Nafion, graphene oxide and ionic liquid composite. *Microchim Acta* 178:211–219. <https://doi.org/10.1007/s00604-012-0811-8>
 35. Ce Z, Zhong J, Li S, Wang H, Wang J, Yan B, Du Y (2017) Fabrication of reduced graphene oxide-bimetallic PdAu nanocomposites for the electrochemical determination of ascorbic acid, dopamine, uric acid and rutin. *J Electroanal Chem* 805:110–119. <https://doi.org/10.1016/j.jelechem.2017.10.020>
 36. Niu X, Wen Z, Li X, Zhao W, Li X, Huang Y, Li Q, Li G, Sun W (2018) Fabrication of graphene and gold nanoparticle modified acupuncture needle electrode and its application in rutin analysis. *Sensors Actuators B Chem* 255:471–477. <https://doi.org/10.1016/j.snb.2017.07.085>
 37. Cui S, Li L, Ding Y, Zhang J, Yang H, Wang Y (2017) Mesoporous NiCo₂O₄-decorated reduced graphene oxide as a novel platform for electrochemical determination of rutin. *Talanta* 164:291–299. <https://doi.org/10.1016/j.talanta.2016.10.109>
 38. Pang P, Li H, Liu Y, Zhang Y, Feng L, Wang H, Wu Z, Yang W (2015) One-pot facile synthesis of platinum nanoparticle decorated reduced graphene oxide composites and their application in electrochemical detection of rutin. *Anal Methods* 7:3581–3586. <https://doi.org/10.1039/c5ay00353a>